Pulse shape discrimination and dark matter search with NaI(Tl) scintillator

G. Gerbier, J. Mallet, L. Mosca, C. Tao, B. Chambon, V. Chazal, M. de Jésus, D. Drain, Y. Messous, C. Pastor

DD

PULSE SHAPE DISCRIMINATION WITH NaI(Tl) and RESULTS FROM A WIMP SEARCH AT THE LABORATOIRE SOUTERRAIN DE MODANE

G. Gerbier, J. Mallet, L. Mosca

DSM/DAPNIA/SPP, C.E. Saclay, F-91191 Gif-sur-Yvette, France

C. Tao

LPCC, Collège de France/ IN2P3 (CNRS), 11, place Marcellin Berthelot, F-75231 Paris, France

B. Chambon, V. Chazal, M. De Jésus, D. Drain, Y. Messous, C. Pastor

IPN Lyon, IN2P3 (CNRS), 43 Bd du 11 Novembre 1918, F-69622 Villeurbanne CEDEX, France

Abstract

An extensive study of NaI(Tl) as a Dark Matter particle detector is presented. Emphasis is put on the response of the detector, both in energy and pulse shape, to all particles interacting in the detector, namely high energy (MeV) photons, low energy photons (X-rays), betas from external radioactivity and neutrons, which induce nuclear recoils.

The initial hope that the shorter decay times of nuclear recoils induced by WIMPs could be statistically separated from Compton interactions is weakened by the fact that low energy X-rays and betas exhibit pulse shapes similar to recoils. As a consequence, any indication of shorter decay time pulses leads to an ambiguous interpretation.

Underground data for the WIMP search were obtained in a low activity environment at the Laboratoire Souterrain de Modane (LSM), with a 10 kg crystal having high photoelectron yield and 2 keV energy threshold. The data contain pulse shapes with decay times shorter than for Compton interactions and are marginally compatible with calibration reference shapes or mixture of these. The Compton rejection efficiency is limited to factors ranging from 3 at 5 keV to 8 at 20 keV.

It is shown that the sensitivity of NaI(Tl) detectors to the cross section of Spin Independent coupling WIMPs is only marginally improved by the pulse shape analysis, while it is mostly determined by the differential energy rate at threshold. The sensitivity to the cross section of Spin Dependent coupling WIMPs is improved by about an order of magnitude by the pulse shape analysis.

1 Introduction

Detecting WIMP particles is a challenge which has motivated a growing number of experiments over the years [1].

The quality of a WIMP detector, that is its sensitivity to nuclear recoils, depends on two main issues : the low activity level of the detector and its environment which determines the low energy differerential rate, and its radioactive background rejection

capability. In the present case of NaI(Tl), the background discrimination is obtained by analysing the scintillation pulse shape of the low energy events.

Concerning the first issue, the main characteristics of the detector (in particular PMTs and light guides) were optimised after the determination of the origins of the radioactivity of the various parts of the detector (section 4).

The second issue constitutes the main focus of this paper. The possibility of nuclear recoil identification using Pulse Shape Discrimination (PSD) was first reported in 1989 by the Saclay group [2].

The measurements of the Sodium and Iodine nuclei recoil scintillation efficiencies obtained in a neutron beam are first reported. Then differences observed between pulse shapes of electromagnetic radiations and nuclear recoils are analysed. The sensitivity of the PSD effect to various experimental conditions is also discussed.

Energy response to less than 10 keV energy electron interactions from external X-ray source (surface interactions) and from Compton induced interactions (volume interactions) are compared. Further pulse shape calibrations using neutron, low energy X-ray and beta sources, performed in low background underground environment, are presented and analysed.

Finally, the underground experiment at LSM is described and the results of the data analysis are discussed. Conservative upper limits on the presence of recoils are then derived and interpreted in terms of WIMP exclusion regions in the mass versus cross section plane. A comparison with other experimental results is performed.

2 Calibrations of NaI(Tl) response to Sodium and Iodine recoils in a neutron beam

The characteristics of NaI(Tl) response to Na and I recoils are essential to interpret data for WIMP search. These two main parameters are :

-the quenching factor or recoil scintillation efficiency, that is the ratio of the amount of light emitted by a nuclear recoil (Na, I) to the amount of light emitted by an electron of the same kinetic energy,

-the time shape difference between the nuclear recoil and the electron pulses. The strong difference observed at MeV energies between alpha and electron decay times [3,4] is indicative of a possible PSD for keV recoiling ions.

2.1 Method and experimental set-up

The method used here is similar to the one used to measure the ionization efficiency in semiconductors as Si [5], Ge [6] and scintillators CaF_2(Eu) [7].

The crystal is exposed to a monoenergetic beam of neutrons inducing elastic collisions on the nuclei of the crystal. The neutrons are produced via the reaction $p+{}^7Li \rightarrow n+{}^7Be$ by a pulsed beam of protons at the Tandem accelerator of Bruyères le Châtel. The scattered neutrons are detected at fixed angles by NE213 detectors with neutron/gamma discrimination capability. Time of flight measurements between the ^{7}Li target, NaI(Tl) crystal and NE213 counters allow a good selection of neutron induced nuclear recoils at a given energy.

The experimental set-up has been described in details in [7]. To avoid multiple neutron interactions, the size of the crystal was limited to 1 inch diameter by 1 inch height. The

crystal was directly coupled to a 2 inch 2232 RTC photomultiplier, providing a large photoelectron yield of 9 pe/keV.

In order to detect low energies, down to 2 keV, a two step trigger was used. After a first discriminator at the single photoelectron pulse height level, a second stage trigger fires when the integrated amplitude over 800 ns is above a threshold of around 1.5 keV. This ensured full trigger efficiency above 2 keV together with a good timing coincidence with NE213 counters.

2.2 Energy response and quenching factors measurements

Calibrations were performed with gamma rays of 60 keV from ^{241}Am and X-rays of 22 and 88 keV from ^{109}Cd sources. X-rays are converted close to the surface of the crystal (less than 1 mm in NaI(Tl) at 60 keV), and the responses may depend on the source position. This effect was measured by varying the position of the source and amounts to at most 4 %. So a systematic error of $\pm$ 2% on the energy calibration was taken into account in the final results.

After applying the appropriate cuts on times of flight and NE213 neutron/gamma discrimination parameters, clean samples of events were obtained. Figure 1 shows the energy spectrum of events selected from a NE213 counter at 102° from the incident neutron beam of 3.3 MeV energy. The low energy peak corresponds to the Iodine recoils and the high energy one to the Na recoils. Figure 2 shows the measured energy (electron equivalent energy or "eee") as a function of the recoil energies for neutron energies of 3.3 Mev for I recoils and 1.3 MeV for Na recoils and scattering angles ranging from 30° to 145°.

The quenching factor is experimentally defined as the ratio of the mean "eee" to the kinematically known recoil energy. This definition is identical to the one given in the introduction provided the response to the electrons is linear, in the range of kinetic energies studied here. This is true within $\pm$8%, as shown in section 3. Quenching factors of 25 % $\pm$ 3% for Na recoils and 8 % $\pm$ 2% for I recoils are obtained as indicated. The errors include the electron response linearity approximation. Notice the quenching factor high values for Na recoils compared to other low A nuclei recoils of 6 % for Ca and 8 % for F nuclei obtained in CaF_2(Eu) [7]. These values agree with measurements of the UKDM group [8].

2.3 Analysis of nuclear recoils and electrons pulse shapes

The second cornerstone of WIMP search with NaI(Tl) is the PSD at keV energies. Like for high energy (MeV) alphas, one may expect that the shape of the pulses are different for nuclear recoils (highly ionising, slow moving particles) and electrons. This investigation is described in the following.

2.3.1 Experimental details

The dependence of the decay time of the scintillation yield with the temperature is a well known effect [3]. The temperature of the crystal was monitored throughout the experiment and kept within $\pm$ 1°C thanks to a Peltier device. The effect of the temperature was actually measured and is reported in section 2.3.4.

Electron induced events were obtained from the Compton interactions of the 662 keV gamma rays (interaction length of 4 cm in NaI(Tl)) from a source of ^{137}Cs. This ensures that the whole volume of the crystal is sampled, like in the case of neutron interactions.

Compton runs were taken in alternance with neutron runs in order to keep the same experimental conditions, especially with respect to the electronics.

Pulses of individual events were digitised by a 200 MHz Transient Digitiser Lecroy module during 1800 ns. This sampling frequency allows to record individual photoelectrons on typically 3 time bins. Figure 3 shows a single 4 keV event where individual photoelectrons are easily identified. Clean samples of events resulted from software cuts to remove time profiles affected by unstability of baseline or electromagnetic noise.

2.3.2 Analysis of Na recoils

Data were analysed in bins of 2 keV energy between 4 and 20 keV. Between 2 and 4 keV, some residual noise from the photomultipier could affect the present results. Most of the runs were taken with a temperature of the crystal of 19°C. Accumulated statistics amount to around 2000 and 6500 evts / 2 keV bin respectively for Na recoils and Compton interactions. We used two methods to compare the two populations.

The first one consists in summing all the event pulse time profiles of a given population per energy slice in order to obtain mean reference pulses. For example, figure 4 shows the pulse shapes in the 12-14 keV bin for the two samples of events. Mean pulses are normalised and amplitude expressed in eV/ns. Errors are calculated from the photostatistics. The two time distributions are integrated with a running sum from the first photoelectron time to 1800 ns later, and normalised to unity. The difference of the two integrated time distributions (Integrated Time Profile Difference or ITPD) is a way to visualise and quantify the difference between two mean pulses.

ITPD curves between Compton and Na recoils are shown on figure 5. The maximum of the curve occurs at around 200 ns which is the crossover time of the two differential profiles and the height gives the amplitude of the PSD effect. The PSD effect amplitude increases with energy from 0.03 at 5 keV to 0.075 at 18 keV.

Would the integration time be only 600 ns (which is roughly 3 times the characteristic scintillation decay time), one can estimate from figure 5 that the maximum amplitude of the PSD effect would be divided by 2. So even if the fraction of the pulse above 600 ns is only 5 to 10 %, this is a significant information. However, increasing too much the integrating window, in a region with a very low density of scintillation photoelectrons, may lead to include PMT random noise which will distort the pulse. A 1800 ns time window was found to be a good compromise.

The other method is based on an event by event parameter characterising the time decay constant. The distributions of this parameter of the two populations are then compared. The parameter is the first moment of the event time differential amplitude profile, that is:

$$< t >= \frac{\sum t_i \, a_i}{\sum a_i} \qquad (1)$$

where a_i is the amplitude of the pulse at the digitised bin "i" of the time t_i , the summation being done from the start of the pulse up to 1800 ns later, as defined above. The parameter <t> is identical to the decay constant in the case of an exponential distribution. As an illustration figure 6a shows the distributions for Na recoils and Compton populations for the 12-14 keV interval. Integrals of the two distributions are normalised to the same area.

However, since the whole information of the pulse is reduced to the first moment of the time profile, higher order moment differences leading to the same <t> will not be accounted for.

Figure 7 shows the variation of the mean value of the <t> distributions with the energy for the two samples. The above mentioned increase of the PSD effect with energy between Compton and recoils is mostly due to the increase of the decay time of the Compton electrons while the decay time of the recoils varies weakly with energy.

We choose a quality factor used by the CDMS group [9] to quantify the rejection capability:

$$Q_{fact} = \frac{\beta(1-\beta)}{(\alpha-\beta)^2} \tag{2}$$

where α (β) is respectively the fraction of recoil (electron) events kept below a given value of the <t> discrimination parameter. The lower the Q, the better the rejection power. For this 12-14 keV energy range, Q shows a minimum at <t> of 190 ns (figure 6b), where $\alpha = 0.43$ and $\beta = 0.11$, which provides a Q value of around 1.

The minimum Q as a function of energy is shown on figure 8. The discrimination power increases with energy (Q down to 0.15 at 22 keV).

The UKDM collaboration, with NaI(Tl) crystals coupled to the PMTs by air light guides [9] obtained a higher Q value of around 2.3 in the 13-16 keV. The reason is the broader time constant distributions due to the poor light collection of their set up leading to a 1.6 pe/keV yield compared to our 9 pe/keV.

The CDMS [10] and EDELWEISS groups [11] state a Q factor of 0.01 in the 10-30 keV range for their Germanium bolometer with ionisation measurement.

2.3.3 Iodine recoils

Iodine pulse shapes were also recorded with statistics about one order of magnitude lower than with Na recoils. The conclusion is that within the present statistical accuracy, recoils from Iodine and Sodium have identical shapes, which is summarised on figure 9, where the mean <t> as a function of energy is displayed for the three samples of Iodine, Sodium and Compton electrons obtained in the same experimental conditions. The 10 ns absolute difference for all samples with respect to figure 7 is due to different experimental conditions (temperature, crystals).

2.3.4 Temperature effect

At ambient temperature, the expected effect of a temperature increase of the crystal is a decrease of the scintillation decay time [3]. This was measured in our experimental conditions both for Compton electrons and nuclear recoils. We have recorded in the 15-26°C range a mean decrease of the mean <t> of about 2.3 ns per °C in the 4-20 keV region. At 10 keV, a systematic error of 1°C on a given data sample corresponds to a 1 % difference in the <t> which is to be compared to the expected 14 % difference of PSD effect at 10-12 keV. The recoils and Compton have identical temperature dependence, so that the pulse shape difference is not significantly affected by temperature variations between 19°C and 26°C.

2.3.5 Summary

In conclusion of this section:

- we have measured a shorter decay time for nuclear recoil scintillation pulses as compared to electron induced ones, the relative difference increasing with energy from 6 to 15% in the 4-20 keV region,

- the pulse shapes of Iodine and Sodium recoils do not differ more than 3 % within the present statistical accuracy,

- the shapes of the nuclear recoils do not change significantly in the 4-20 keV range while the decay time of the electron increases with energy,

- the temperature induces a decrease of the decay time of about 1 % /°C . The temperature stability of an underground experiment have to be better than 1 °C to allow the detection of a 10% component of recoils in a Compton background.

3 NaI(Tl) response to low energy electrons

From the literature [3], the non linearity of NaI(Tl) between 2 and 60 keV is not expected to be greater than 20 %. The detectors were designed to allow calibration from external sources down to a few keV, through a thin 5 mm diameter window made with MIB (Multi Interlaminal Barrier, composed of a polyamide film, adhesive and high purity Aluminum) of 168 μm thickness, in the copper housing. When shining the crystal with ^{109}Cd (22 keV) and ^{241}Am (60 keV) sources, a good linearity is observed in this energy range. However, calibrations performed with a ^{55}Fe source show large non linearity, namely the 5.9 keV peak is observed at around 4.4 keV. This was observed for many different crystals and is not compatible with response curves obtained in the sixties with small cleaved crystals (continuous curve of figure 10).

The hypothesis that this non linearity is due to a surface effect (grinded surface for the presently used crystals) was checked by performing for the same crystal a Compton diffusion experiment with high energy photons (4 cm interaction length) sampling the whole volume. The photons were produced by a ^{137}Cs source (662 keV), scattered in the NaI crystal and detected by a Ge detector at various angles. Expected energies deposited in NaI calculated from kinematics were cross checked by measuring the full absorption peak of the scattered gamma in the Germanium detector. Then the ratio of the mean measured NaI energy to the expected energy is calculated at various angles and plotted as a function of the expected energy. The non linearity observed at 5 keV corresponds to 97 % of the response at 60 keV (figure 10), compatible with previous results from literature but not with ^{55}Fe calibration.

The conclusion is that low energy calibration with ^{55}Fe source is meaningless with our experimental conditions, and we will assume in the following a linear behaviour between 0 and 60 keV.

4 Underground measurements

4.1 Experimental set-up

The present data were collected at the Laboratoire Souterrain de Modane, in the Alps, along the Frejus road Tunnel between France and Italy, with an overburden of 4800 mwe. The detector used was a 9.7 kg parallepipedic 10 cm by 10 cm by 25 cm NaI(Tl) crystal

grown and equipped by the CRISMATEC company, using low activity materials we had selected. The copper housing is equipped with a thin MIB window (168 μm) on one side of the crystal to allow for low energy calibrations.

The crystal was coupled on both ends with a 10 cm long quartz light guide to a low activity 3" diameter EMI photomultiplier. In spite of an important low activity development by EMI, these PMTs remained the most active component of the NaI(Tl) crystal nearby environment. The length of the light guide was set so that the contribution of the PMTs activity remains less than 10 % of the total counting rate. The detector was surrounded by a very low activity archeological lead shield of 10 cm itself inside a low activity plexiglass box through which nitrogen was flushed at an overpressure of few mbars to avoide the radon. The box was housed in a large castle made of 15 cm of low activity lead and the free space was filled with expanded polystyrene.

Amplified outputs of the signals were discriminated at the photoelectron level and then put in coincidence to build the first level trigger. A second level trigger kept only pulses corresponding to an energy greater than 2 keV. Pulses were digitised and processed in exactly the same way for all the calibration and data samples as described in previous section. The measured photoelectron yield was about 7 pe/keV.

Calibrations were performed thanks to a dedicated system, allowing to introduce the sources close to the crystal trough the plastic box and the lead shield.

4.2 Calibrations

The energy is known from the response of the detector to the 60 keV line of a ^{241}Am source. The energy resolution was $\sigma/\mathrm{E} = 2.8/\sqrt{(E)}$, with E in MeV. The overall stability was measured with the 60 keV line throughout the time of the experiment and was found to be $\pm$ 2.5 %.

4.2.1 Compton reference pulse shape

The PSD Compton calibrations were performed with a ^{137}Cs source, before, during and after the period of data acquisition, with statistics about 5 times larger than the data. The energy of this line (662 keV) is high enough to ensure that the volume is uniformly illuminated and that the fraction of events at energy less than 20 keV coming from multiple Compton interactions is less than 2 %. This point is important because the shapes of the Compton profiles vary significantly with energy. The spectrum below 30 keV is flat.

4.2.2 Neutron source reference pulse shape

A recoil calibration with a neutron source (^{252}Cf) was performed in situ. Counting rates from the neutron interactions largely dominated the electromagnetic rate.

Due to the large size of the crystal, multiple interactions could not be excluded. However, the shapes of the recoils do not change with energy (section 4), which means that, for example, a pulse of 10 keV induced by two interactions of 5 keV gives the same shape as a single 10 keV scattering.

Amplitudes of the PSD effect between Compton and neutron induced recoils, shown by the ITPD curves (figure 11) and their dependence with energy are found to be very comparable to those obtained in the beam calibration experiment (figure 5). This validates the underground source calibration. The amplitudes of the ITPD (see definition at section

2.3.2) range from 0.03 to 0.075. The reference shapes used in the following come from this neutron source calibration.

4.2.3 Low energy X-rays and β

Calibration with a ^{55}Fe source (5.9 keV peak) not only has shown a strong non linearity (section 3) but also the shapes of the pulses were found to be quite different from Compton interactions. We performed further calibrations with higher energy X-rays from an external source of ^{241}Am shining through the MIB window. Due to the moderate energy resolution of NaI(Tl), the multiple X-rays from the ^{241}Am source give a smooth continuum below 20 keV. Surprisingly, the ITPD of X-rays relative to Compton population (figure 12) are very similar to the nuclear recoil ones, though the amplitudes are lower (from 0.035 to 0.05 compared to 0.03 to 0.075 for recoils) and the variation with energy is different.

We also performed a calibration with β particles from an external source of ^{60}Co. ITPD relative to Compton population (figure 13) show the same tendency with lower amplitudes (from 0.02 to 0.025).

All these results indicate that any residual radioactive surface contamination, either on the surface of the crystal or of the optical reflector sheet in contact with the crystal, or of the copper housing, may induce low energy X-rays and/or β which can nearly fake a recoil contribution.

4.3 Data

Data for WIMP search were accumulated during 83 days. The temperature excursions did not exceed $\pm$ 1°C around 19°C. A few runs with larger deviations were removed from the data.

Though the PMTs were selected for their low electronic noise, which never exceeds 200 Hz, and the trigger selects PMTs firing in coincidence, the counting rate at energy lower than 6 keV is still dominated by the photomultiplier noise, by a factor about 7 over the scintillation pulses. Nevertheless, the noise exhibits a pulse shape, much more concentrated at early times than the true NaI(Tl) pulses. It was removed by software cuts for each event, mainly on two parameters, the mean amplitude per time bin, and the asymetry between the two PMT pulse heights.

The quality of the selection of the events in the 2-5 keV region is illustrated on figures 14. Figure 14a shows the distribution of the mean amplitude per time bin for all the events and for the PMT noise anti-selected events. Assuming a gaussian for the noise, as suggested by the right side of the distribution, one finds 15% of the data are misassigned noise events. On the other hand, comparison of selected data events with true Compton events (Figure 14b) show little contamination of noise in the selected data events (less than 5%).

Therefore, the selection discussed above keeps more than 85% of the true NaI(Tl) pulses in the 2-5 keV bin and the efficiency reaches 100% above 6 keV.

4.3.1 Low energy data spectrum

The low energy (less than 20 keV) experimental differential rate obtained as explained above is shown on figure 15, together with the rough acquisition rate, and the rate corrected for the losses due to the cuts.

The selection guarantees that the increase of rate between 2 and 5 keV relative to the rate above 5 keV originates from true scintillation pulses. A possible origin could be the 3 keV X-rays from ^{40}K decays inside the crystal. The counting rate above 5 keV is nearly constant and equal to 2 evts/kg/keV/day up to 20 keV.

4.3.2 PSD analysis

The studied energy range is 4-20 keV. Data below 4 keV were not considered because of the residual PMT electronic noise contamination. The ITPD (see section 2.3.2) between data and the Compton population was built in the same way as for the calibrations (figure 16). They are not flat. They show systematic deviation on the negative side for all energy intervals, that is data have shorter decay times than pure Compton, like recoils or betas or X-rays.

The maximum deviation of this ITPD from zero expected from statistics at 90% CL was calculated. The result is shown on figure 17, for the 10-12 keV energy bin, together with the data-Compton ITPD. Data are definitely not compatible with pure Compton.

On the other hand, the ITPDs between various Compton runs are found to be marginally compatible within errors and show typical deviations at 200 ns from pure statistics by a factor 2 on the positive and negative side. However, data show deviations from the Compton population by a factor 8 definitely higher than the inter-Compton deviations. Data exhibit a shape which is roughly comparable to recoils/beta/X-ray ones at times lower than 600 ns, but the overshoot at higher times is not compatible with any shape expected from calibrations. Would we have only considered the 0-600 ns window (or only the maximal amplitude of the ITPD), such differences would not have been noticed. This suggests the presence of another population of events or systematic effects. After a careful scan of low energy events, we did not find a population of pathological events which could account for this effect. We checked the PMTs, the preamps, the electronics (digitisation), and also the triggering and analysis procedures, but no satisfactory explanation came up.

Assuming that the first part of the pulse indeed reflects a contribution from recoil/beta/X-ray, the effect of overshoot could empirically be accounted for by an additional quasi flat scintillation component of 0.2 photolectrons per event, with a time constant greater than 1 μs but lower than 50 μs. The PMT noise rate is too small to account for such an effect. A speculative interpretation consists of a relaxing phenomena of internal strains whenever there is an excitation of the crystal by a particle interaction, only observed in case of very low counting data rates but hidden in runs with high counting rates.

We made an experiment with a wood shield of 10 cm around the lead castle, and found no difference with the previous data, discarding the ambient neutron background hypothesis.

We could not prove either the flat component hypothesis nor the X-ray/beta hypothesis, so we adopt in the following a conservative approach.

4.3.3 Rejection of the Compton background

We previously showed that the mean Data pulse shape (D) is not fully described by a linear superposition of mean Compton (C) and mean Recoil nucleus recoil (R) shapes. This effect limits the sensitivity of a two populations PSD rejection analysis but still upper

limits on the fraction of recoils can be set, because the data are not fully compatible with recoils alone.

These limits were estimated using various estimators such as chi-square (χ^2), likelihood and Kolmogorov-Smirnov estimators. All of these estimators lead to comparable results even if robustness and sensitivity vary slightly. We restrict ourselves here to a standard χ^2 metrics between a shape reference and the hypothesis defined as

$$\text{Hyp (R, C or D)} = \alpha * \text{R} + (1\text{-}\alpha) * \text{(C or D) with } 0 < \alpha < 1$$

The parameter α is the fraction of recoils R, $1/\alpha$ is the rejection factor and $(1\text{-}\alpha)$ is the fraction of non-recoils which can be removed to estimate the upper limit of the WIMP nucleon cross section.

The distribution of the estimator results from 1000 draws on the time bin shape distribution with a 3 sigmas gaussian error, so the distribution and its statistical interpretation are independent of any assumed estimator distribution.

The sensitivity resulting of statistical errors is measured taking the D shape as the reference shape and using the same D shape distribution in the hypothesis Hyp(R,D). The mean estimator is then a monotonically increasing function of the R fraction α as illustrated by figure 18 for a given energy interval. The R fractions α associated to a 90% confidence level are reported as a function of energy in table 1, column "stat". The α fraction ranges from 13% at 4-6 keV down to 4% above 12 keV. This sets the best statistical limits, with the present running time and detector mass.

However, as anticipated from previous remarks, the estimator built between the Data and a mixture of recoils and Compton, Hyp(R,C) does not exhibit the same behaviour. A small fraction of R decreases the χ^2 mean value, that is, the data are compatible with a contribution of shorter decay times but no value of α provide a χ^2 value close to one, that is, the data are not compatible with a contribution of only Compton and nuclear recoil events. Assuming the behaviour of this estimator is close of a χ^2 type, the maximum contribution of the recoils in the Data is evaluated by renormalizing the χ^2 to one at minimum of this function (shown on figure 18). The recoil fraction at 90% of confidence level then varies from 35% at 4-6 keV down to 12% above 15 keV. This is reported in the column "stat+syst" of table 1. These maximal fractions of signal in the data are then applied to the initial energy distribution to get the maximum event rate which cannot be excluded as being WIMP interactions (table 2).

Table 1: *Sensitivities to nuclear recoils : maximum fraction (90 % CL) of recoils in the data per energy interval.*

Experiment	LSM	LSM	DAMA	UKDM
Exposure (kg.day)	805	805	4123	1003
Energy interval	only stat	stat+syst	only stat	only stat
4-6 keV	0.13	0.35	0.12	0.18
6-8 keV	0.09	0.29	0.08	0.08
8-10 keV	0.08	0.28	0.036	0.06
10-12 keV	0.06	0.16	0.022	0.04
12-14 keV	0.04	0.14	0.017	0.03
14-16 keV	0.04	0.12	0.012	0.03
16-20 keV	0.04	0.12	0.012	0.03

Table 2: *Raw rates and maximum rates (evts/kg/keV/day) at 90 % CL for a WIMP signal, using the α fraction of the "LSM stat+syst" column of table 1*

Energy interval	Raw rate evts/kg/keV/day	Upper limit from WIMP's evts/kg/keV/day
2-3 keV	9.8	—
3-4 keV	6.5	—
4-6 keV	2.84	1.00
6-8 keV	2.21	0.64
8-10 keV	2.17	0.61
10-12 keV	2.30	0.37
12-14 keV	2.49	0.35
14-16 keV	2.48	0.30
16-20 keV	2.00	0.24

4.3.4 Comparison with other experiments

Our sensitivity to recoil, expressed as the maximum fraction of recoils which can be accomodated in the data, are compared in table 1 with published values from two other experiments. The theoretical statistical rejection factor obtained with the PSD goes like $\sqrt{(N/Q)}$ where N is the total number of events accumulated, proportional to the exposure (mass * time), and Q is the discrimination quality factor, which depends on the photoelectron yield and the method of analysis.

The UKDM experiment [9] has comparable exposure of 1000 kg.day. With much lower photoelectron yield/keV, that is with a priori less good separation between Compton and recoils, rejection factors are nevertheless comparable to our statistical one. A possible reason consists in the smoothing of the discrimination parameter from an energy bin to another, performed by the authors, which allows to decrease the errors on these parameters, and thus to obtain a better statistical separation quality.

A second comment is relative to the high energy part of their data, where 2 data points are respectively at 2.5 and 3.2 sigmas aways from zero, which is quite statistically unlikely considering the total of 8 data points. This was noticed by the authors, "the positive deviation near 20 keV cannot be significant as a nuclear recoil signal, since the elastic nuclear recoil spectrum must always fall with increasing energy". This is true, but this positive deviation is an indication of systematic effects, which could also be present at lower energies, and was not taken into account.

The Gran Sasso DAMA group uses detectors built from the same material and with the same protocol as ours [12]. With 4 times the exposure of the present experiment, they get statistical rejection factors better by about a factor 2, as expected.

The energy spectra of their crystals do not show the low energy 2-5 keV peak, that we have observed in our present data, and in many other prototype crystals. The lowest rate among the detectors at 2.5 keV is around 0.5 evts/kg/keV/day, while we measure a rate of 10 evts/kg/keV/day. There is no indication of a decrease with time of this peak at low energy in our data. Strong cuts are applied in the DAMA analysis to remove the PMT noise between 2 and 12 keV, leading to an efficiency of 30-40 % only at low energies. As

pointed out in the above analysis, with similar detectors, noise rejection can be performed with efficiency of 85 % in the 2-5 keV region. The data analysis of this low energy region is crucial as it determines the sensitivity to Spin Independent coupling WIMPs, as shown in next section. Above 12 keV, both experiments find similar rates within a factor 2.

5 Limits in the WIMP mass cross section plane

We have adopted a procedure similar to the one of ref [13], in order to extract limit cross section versus WIMP mass contours. For a given WIMP mass, the recoil energy differential spectrum can be calculated and the lowest cross section to which the experiment is sensitive is given by the maximum signal which cannot be excluded in the experimental spectrum at any energy. This upper limit results of the PSD analysis whenever possible.

The expected differential energy recoil spectra of WIMPs on nuclei depend on three sets of assumptions: astrophysical parameters (local density, velocities), nuclear physics (matrix elements, spin factors, form factors) and instrumental conditions (energy threshold, detector resolutions and scintillation efficiencies).

The scintillation efficiencies used are respectively 0.25 and 0.08 for Na and I (see section 2.2). The detector energy resolution was taken into acount.

5.1 Astrophysics assumptions

In order to compare with other experiments, we made the following simplifying assumptions:
- WIMPS are distributed in a spherical halo with a local density in the solar neighbourhood, assumed to be 0.3 GeV/cm^3,
- their velocities follow a Maxwellian distribution in the Galactic frame with a WIMP average velocity w = 300 km/s. This distribution is truncated at 800 km/s, the escape velocity.

5.2 Factors related to nuclear physics

For coherent interactions, we used the Engel form factor [14]. For the spin dependent case, we included the spin factors calculated in the odd group model of Ellis and Flores [15] - ^{23}Na: 0.041, ^{127}I: 0.023 and ^{73}Ge: 0.065 - and a spin form factor with a Bessel function shape as for the mass form factor of Engel (1991) in reference [16]. The spin form factor introduces a negligible correction for Na.

5.3 Results and discussion

To compare these results with those obtained with different nuclei, we renormalize cross sections to cross sections on proton. They are reported as exclusion contours in the WIMP mass versus WIMP-nucleon cross section plane.

In the case of Spin Independent coupling interactions the cross section is scaled according to A^2. Results are shown on figure 19. Recoils occur mostly on Iodine, the expected recoil energy distribution is very steep and most of the signal is below 4 keV, where the PSD is inefficient. So the PSD brings little improvement, as shown by the curves "PSD" and "No PSD". The sensitivity comes mostly from the differential energy rate at the lowest energy. This is illustrated by the curve "flat background down to 2 keV" obtained by

substracting the 3 keV peak of our data, at a rate of 10 evts/kg/keV/day, and extrapolating the rate of 2.2 evts/kg/keV/day at 6 keV constant down to 2 keV. However, there is no justification in subtracting this peak, firstly because we do not see clearly the drop of the peak on the left side and secondly because this is precisely the region where Iodine recoils may be present. The better results obtained by the DAMA experiment does not come from better statistical rejection factors above 4 keV but from the lower rate of 0.5 evts/kg/keV/day at the threshold energy of 2.5 keV, due to the absence of the peak we observe.

In figure 20 are shown the exclusion plots in the case of Spin Dependent coupling interactions obtained by the present experiment with NaI, with and without the PSD.

6 Conclusions

Accelerator experiments performed in this work with well defined neutron energy and scattering angles have demonstrated the possibility of partially discriminating nuclear recoils from electron recoils in NaI(Tl) by pulse shape analysis. Nuclear recoils exhibit shorter decay times than Comptons, and the amplitude of this difference increases with energy.

Similar conclusions were reached with neutron sources which turn out to be valuable subsidiaries in deep underground environment.

However, surface interactions induced by X-rays or betas from outside the crystal, induce pulse shapes similar to that of nuclear recoils. Independently of the neutron hypothesis, this raises the problem of the interpretation of any possible signal seen by this kind of detector with a pulse shape analysis.

Finally, a WIMP search was realized using data from an exposure of a 9.7 kg crystal performed during 83 days in a low radioactive background environment at the Laboratoire Souterrain de Modane. The measured total rate of 2 evts/kg/keV/day above 5 keV is comparable to recently published results from other experiments. Hovewer, the rate of 10 evts/kg/keV/day at an effective energy threshold of 2 keV, is higher than that reported by other experiments using very similar detectors.

Data pulse shapes exhibit shorter decay times than expected from pure Compton. However they are marginally compatible with any contribution of recoils, X-rays or betas. We conclude that systematic effects distorting the shapes, observed in the present experimental conditions, limit the power of this kind of analysis. Conservative upper limits were derived from the analysis of a 805 kg.day exposure, where it was shown that systematical errors are already dominant over statistical ones.

Exclusion regions in the WIMP mass versus WIMP-nucleon cross section plane were obtained. It was shown that the PSD is efficient to increase the sensitivity to Spin Dependent coupling WIMPs but brings little improvement in the exclusion zone for Spin Independent coupling WIMPs. In this last case, the sensitivity is mostly determined by the rate at the lowest energy.

For all these reasons, any increase of the mass and/or time, even by orders of magnitude, with the present performances of NaI(Tl) detectors, cannot improve the sensitivity of such experiments. Better discrimination power and/or much lower radioactive background detectors are the two ways to improve the sensitivity to WIMP search.

Acknowledgements

It is a pleasure to thank the LSM staff for providing support to the running of the experiment. Previous contributions from E. Gaillard to the radioactivity measurements, E. Sauvan to the Compton scattering experiment with a Germanium detector and I. Prostakov for the development of specific signal/background separation algorithms, are gratefully acknowledged.

References

1. L. Mosca, Proc 31st Rencontres de Moriond (Edition Frontieres 1996), 53
2. G. Gerbier et al., Proc 25th Rencontres de Moriond (Edition Frontieres 1990), 469
3. J.B. Birks, Theory and practice of scintillation counters, Pergamon Press,Oxford 1964.
4. C. Bacci et al., Phys. Lett. **B293** (1992), 460.
5. G. Gerbier et al., Phys. Rev **D 42** (1990) 3211
6. Y. Messous et al., Astr. Phys. 3 (1995) 361,
7. C. Bacci et al., Astr. Phys. 2 (1994) 117
8. N.J.C. Spooner et al. Phys. Lett. **B 321** (1994) 156-160
9. P. F. Smith et al., Phys. Lett. **B 379** (1996) 299
10. R. J. Gaitskell et al., Proc. of 7th International Workshop of LTD 7, (1997), 221
11. D. L'Hote et al., Proc. of 7th International Workshop of LTD 7, (1997), 237
L. Berge et al., Proc of TAUP97, LNGS, to be published in Nucl. Phys. B, astro-ph/9801199
12. R. Bernabei et al., Phys. Lett. **B 389**(1996) 757
13. A. Bottino et al., Phys. Lett. **B 295** (1992) 330
14. Engel, Pittel, Vogel, Int. J. Mod. Phys. **E1** (1992) 1
15. J. Ellis and R.A. Flores, Phys. Lett. **B263** (1991), 259.
16. J. Engel, Phys. Lett. **B 264** (1991) 114
17. M. Beck et al., Phys. Lett. **B 336** (1994) 141

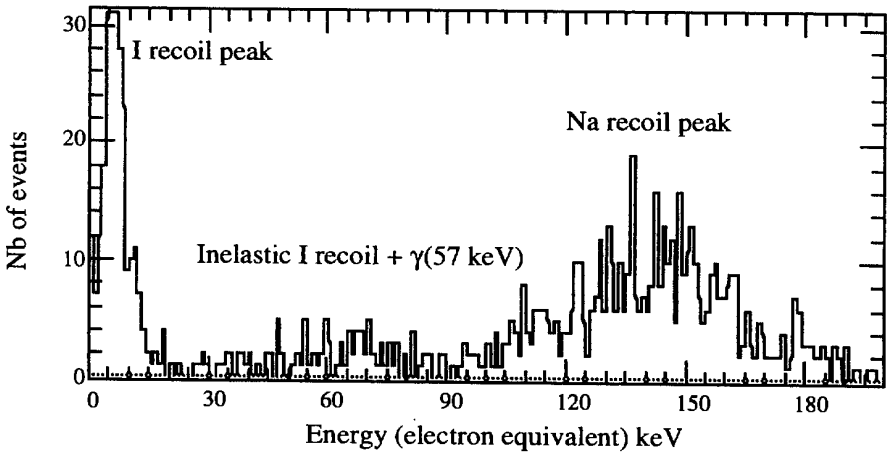

Figure 1: *Energy (electron equivalent) distribution of the recoil events selected at a fixed neutron scattering angle. Peaks due to Iodine and Sodium recoils can be easily oberved.*

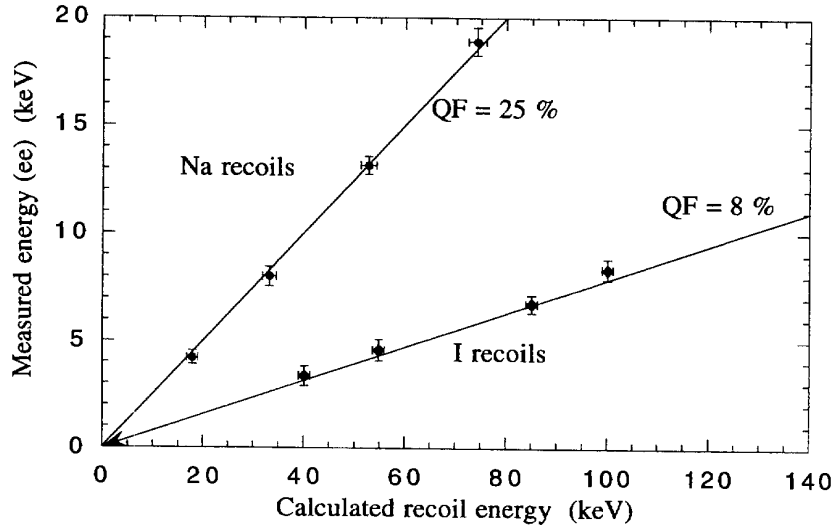

Figure 2: *Measured recoil energy in NaI(Tl) as a function of the true real kinetic energy of the recoils on Na and I nuclei.*

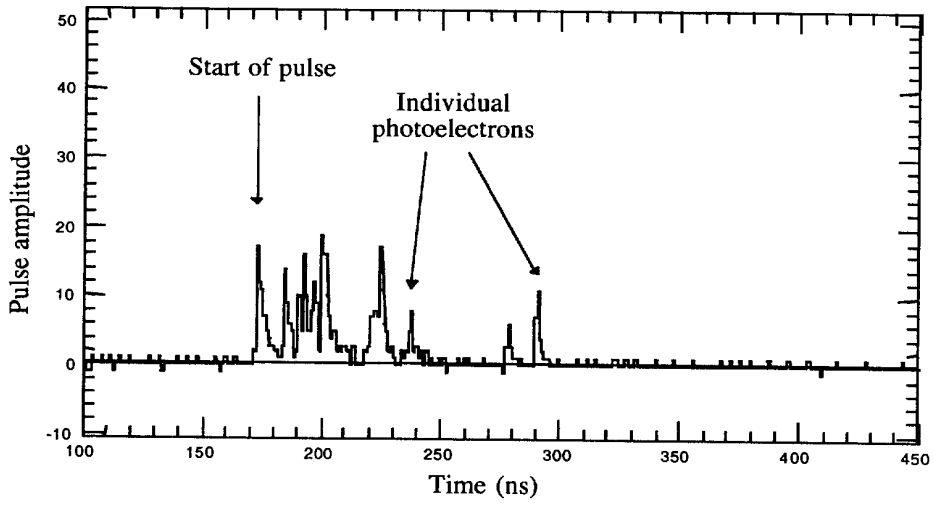

Figure 3: *Example of the time profile of a 4 keV NaI(Tl) pulse : individual photoelectrons are easily identified.*

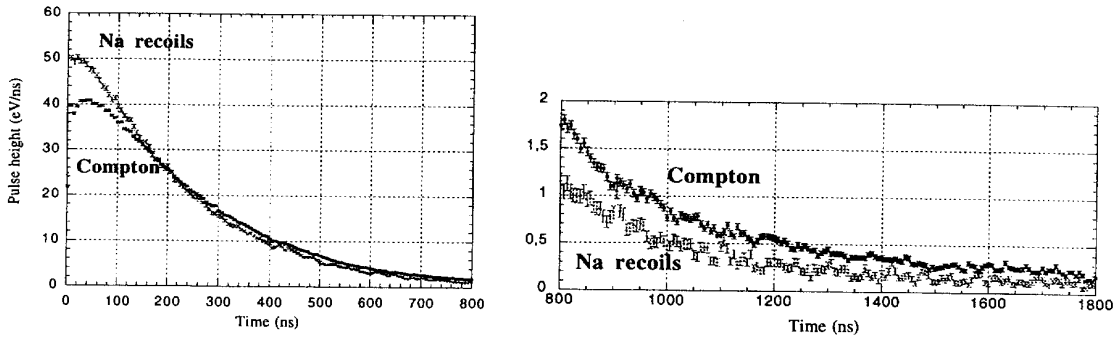

Figure 4: *Reference pulses for Compton and Na recoil events for the 12-14 keV equivalent electron energy bin up to 1800 ns. The integrals up to 1800 ns are normalised to the same area.*

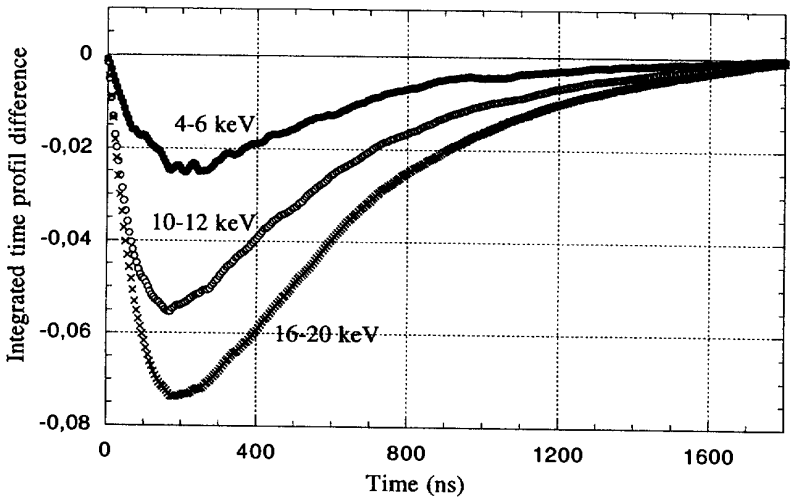

Figure 5: *Integrated time profil difference between Compton and Na recoils (neutron beam, 1" by 1" crystal) for 3 energy bins 4-6, 10-12 and 16-20 keV. The amplitude of the difference (defined at 200 ns) increases with energy.*

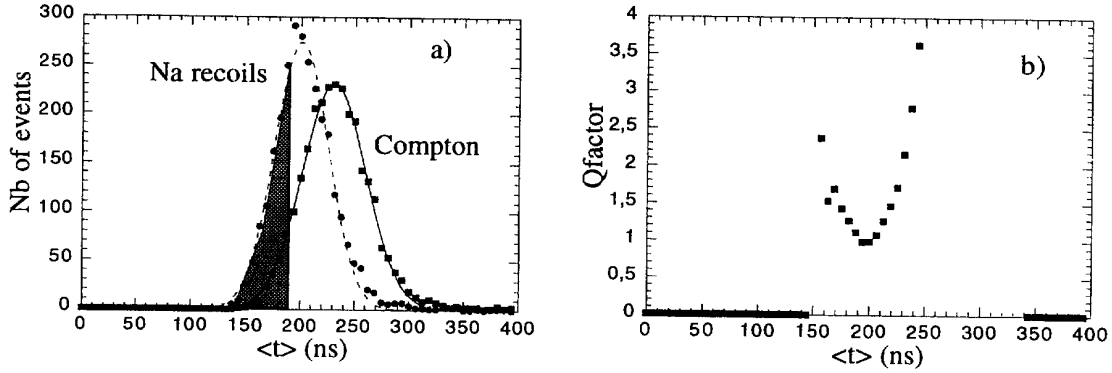

Figure 6: *a) distribution of the <t> variable for the recoils and Compton populations in the 12-14 keV bin .The 190 ns cut gives α=0.43 and β=0.11, b) variation of Q with the <t> cut.*

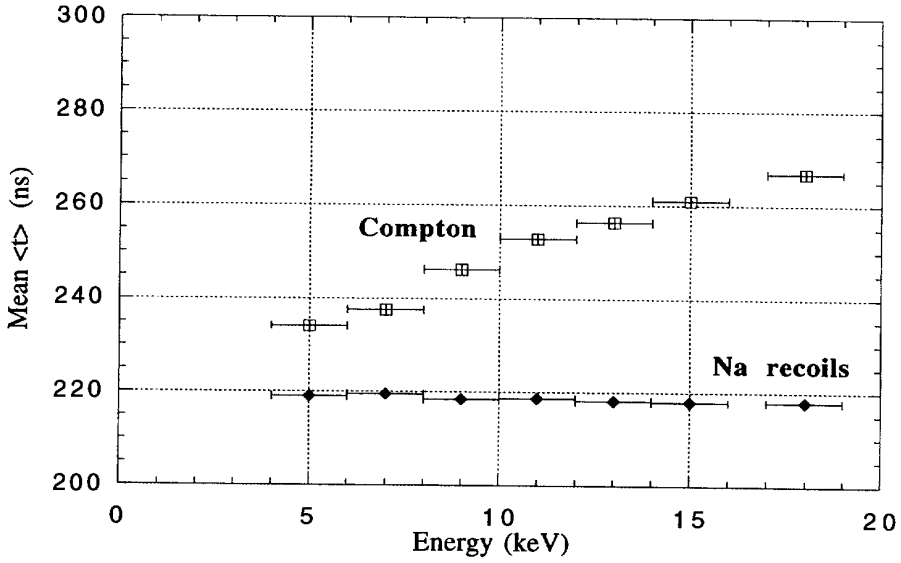

Figure 7: *Mean values of the <t> distributions for the two populations of Compton and Na recoil events.*

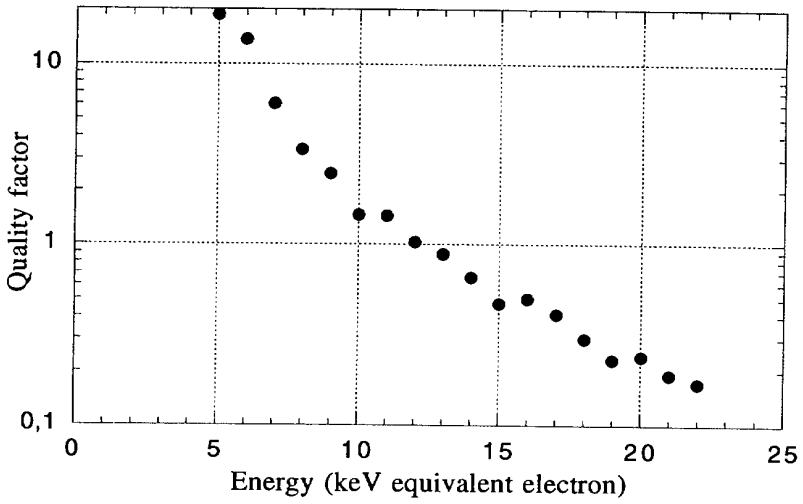

Figure 8: *Variation of the discrimination quality factor Q as a function of energy.*

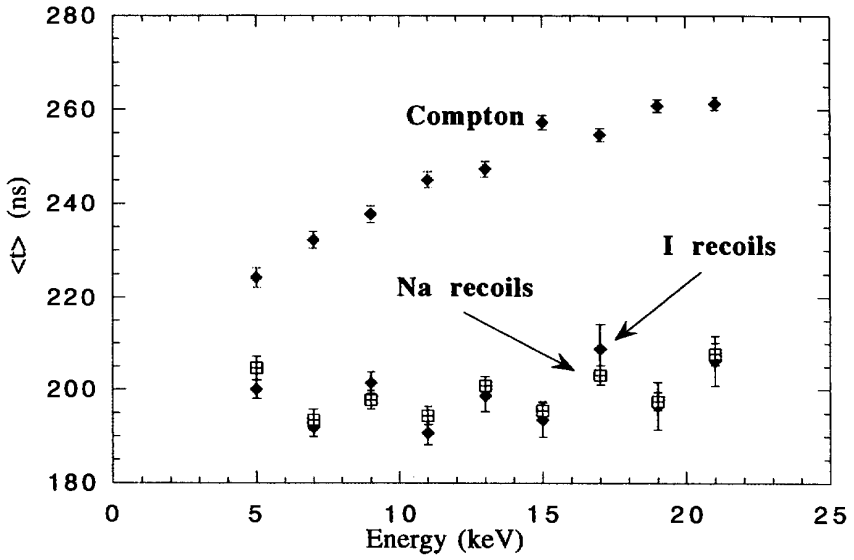

Figure 9: *Variation of the mean <t> variable for the Sodium, Iodine recoils and Compton populations (neutron beam, 1" by 1" crystal).*

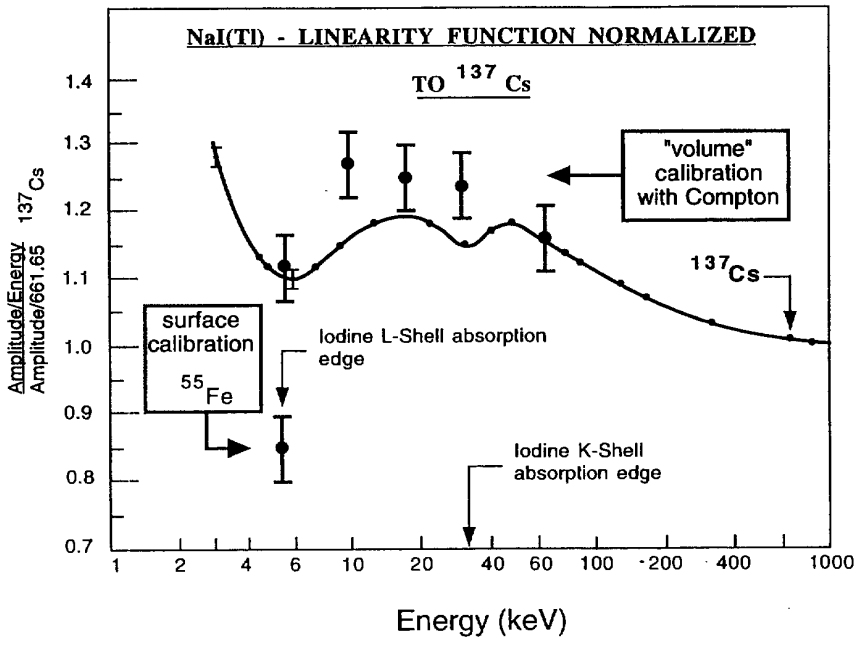

Figure 10: *Variation with energy of the response (surface and volume for low energy) of NaI(Tl).*

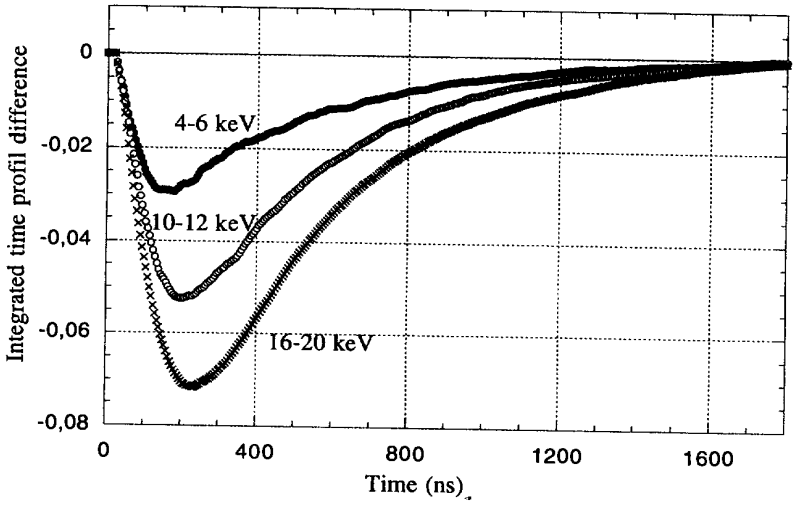

Figure 11: *Integrated time profil difference between Compton and Na recoils (neutron source, 9.7 kg crystal).*

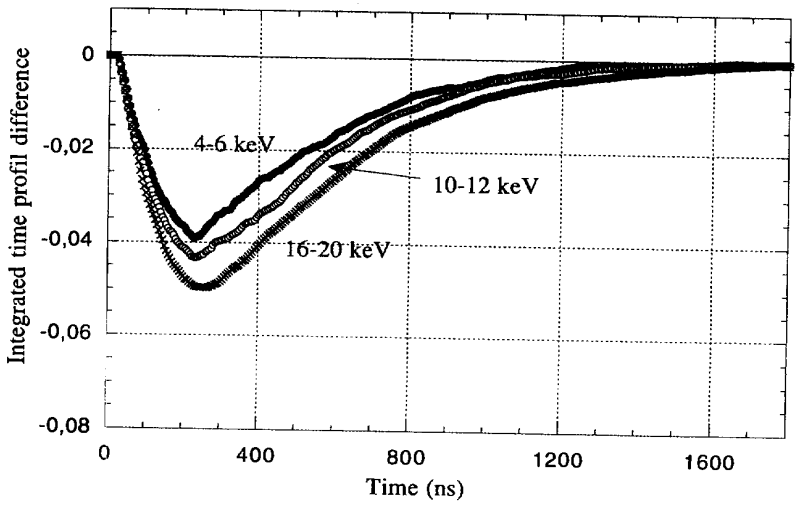

Figure 12: *Integrated time profil difference between Compton and X rays from an external ^{241}Am source.*

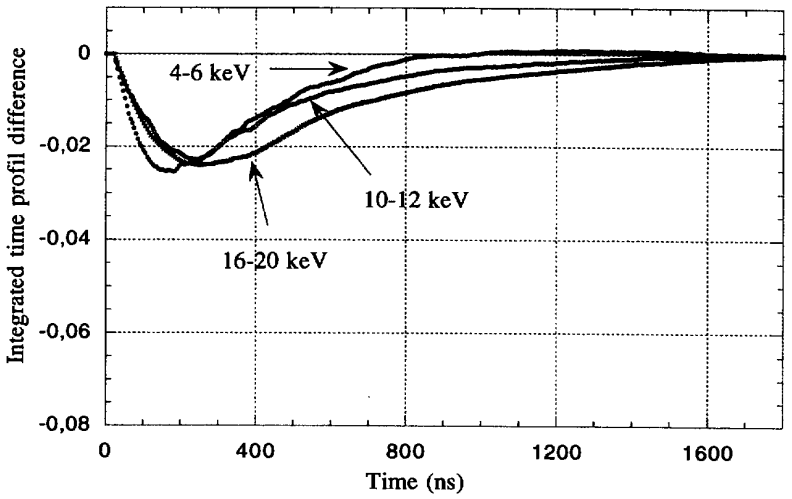

Figure 13: *Integrated time profil difference between Compton and betas from an external ^{57}Co source.*

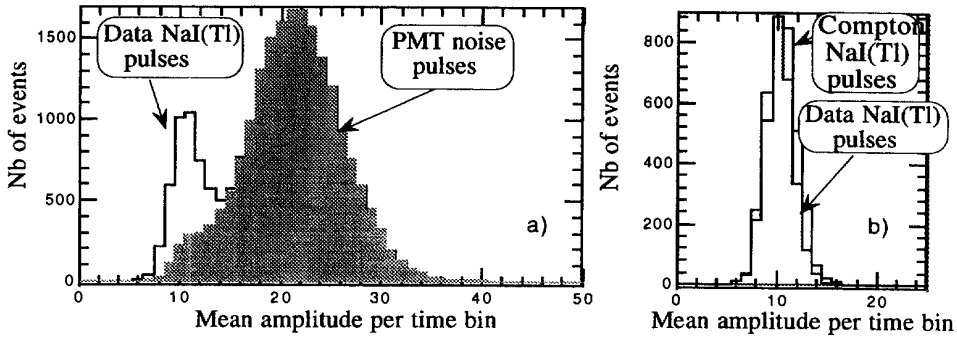

Figure 14: *Noise discrimination parameter (mean amplitude per time bin) distributions for the 2-5 keV bin a) all events, noise (shaded) and data (blank) selected events b)selected data and compton events.*

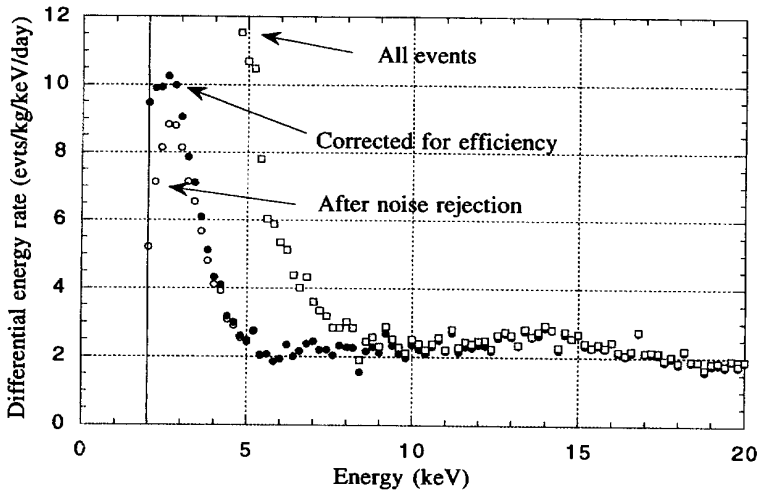

Figure 15: *Low energy spectra of data acquired during 83 days : raw rate, after cleaning of noise, and correction for event losses.*

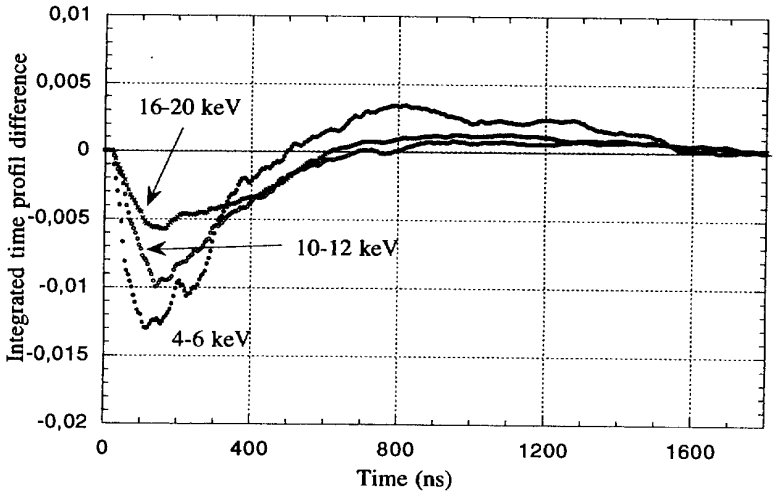

Figure 16: *Integrated time profil difference between Compton and data acquired during 83 days.*

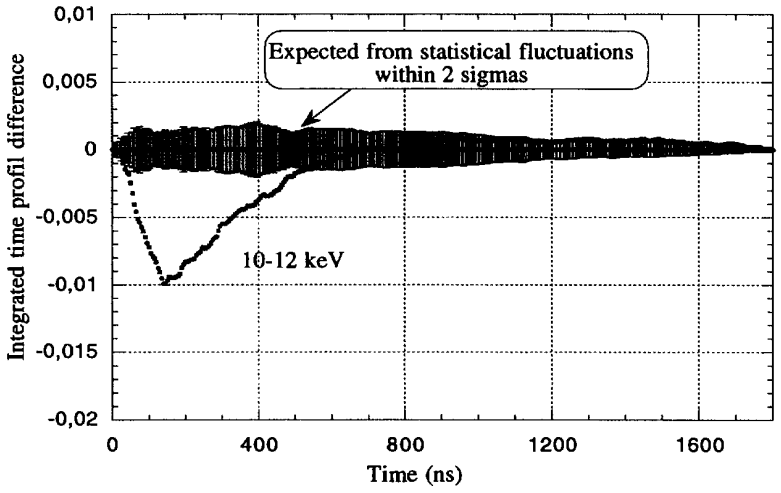

Figure 17: *Integrated time profil difference between Compton and data together with the expected statistical fluctuations zone for the 10-12 keV energy bin.*

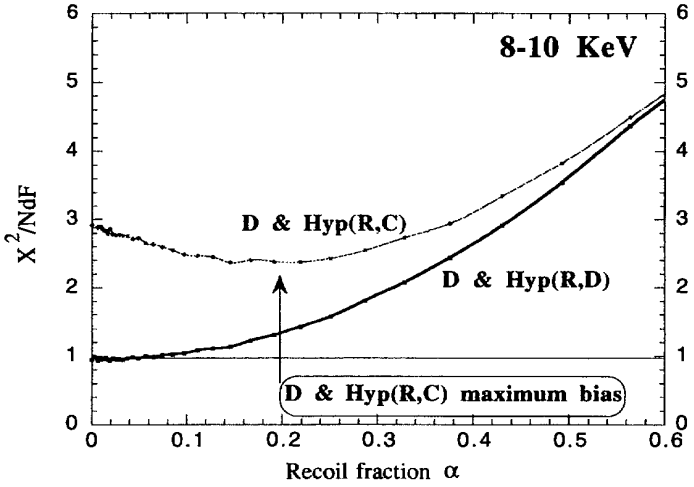

Figure 18: *Variation of χ^2 between the Data population shape and hypothesis built of mixtures of populations R (Nuclear recoils) and C (Compton), D (Data) for the 8-10 keV energy slice. See text for details. When comparing Data and a mixture of Recoils/Compton no value of recoil fraction provides a χ^2 close to 1.*

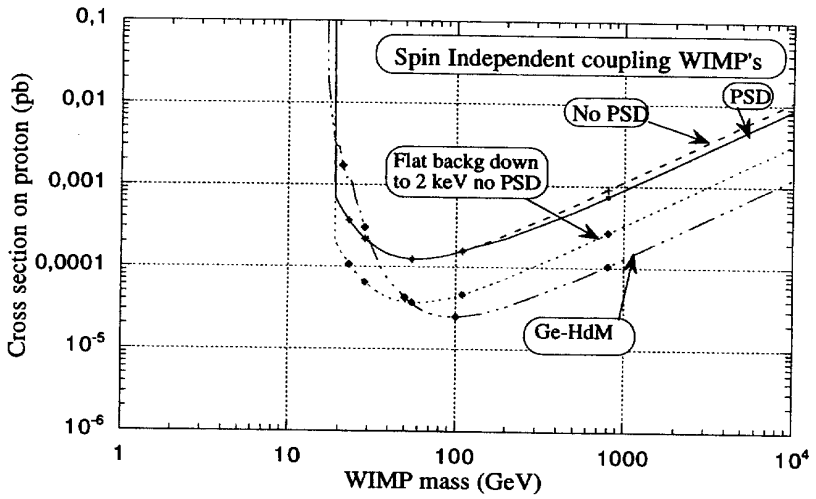

Figure 19: *Exclusion diagrams in the WIMP Mass/(WIMP-nucleon cross section) plane, for Spin Independent coupling WIMP's. Little improvement comes from the PSD (curves "PSD and "No PSD") because recoils occur mostly on Iodine, at energies below 4 keV, where the PSD is not efficient. The sensitivity to the rate at the threshold is illustrated by the curve "flat back down to 2 keV" obtained by extrapolating the rate of 2.2 evts/kg/keV/day at 6 keV constant down to 2 keV (See text). Also shown for reference is the exclusion curve from the Heidelberg-Moscow experiment [17].*

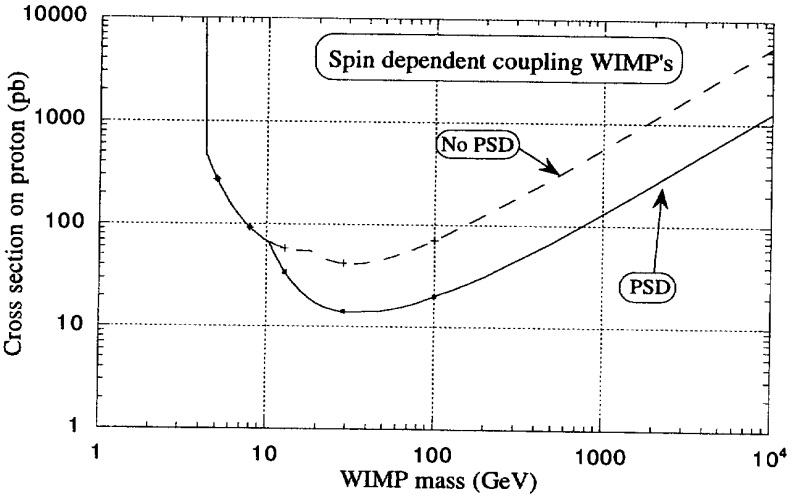

Figure 20: *Exclusion diagrams in the WIMP Mass/(WIMP-nucleon cross section) plane, for Spin Dependent coupling WIMP's. Here is clearly seen the importance of the PSD.*